Journal of Materials Chemistry A

Accepted Manuscript

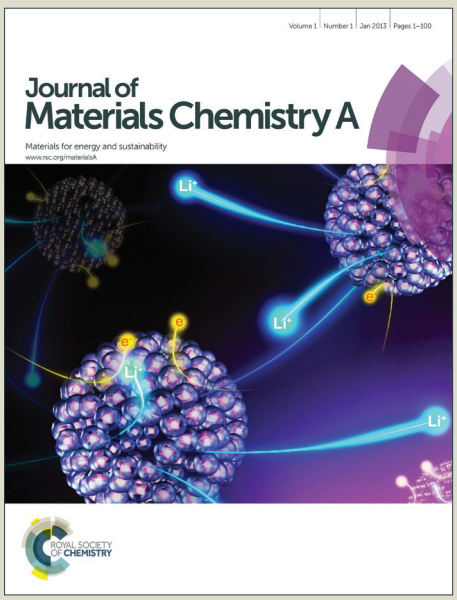

ROYAL SOCIETY OF CHEMISTRY

www.rsc.org/materialsA

Catalytic materials for the hydrogenolysis of glycerol to 1,3-propanediol

Yoshinao Nakagawa*, Masazumi Tamura and Keiichi Tomishige*

Department of Applied Chemistry, School of Engineering, Tohoku University, 6-6-07 Aoba, Aramaki, Aoba-ku, Sendai, Miyagi 980-8579, Japan

* Corresponding authors.

E-mail: yoshinao@erec.che.tohoku.ac.jp; tomi@erec.che.tohoku.ac.jp

Tel&Fax: +81-22-795-7215

Abstract

Recent progress in catalyst development for glycerol hydrogenolysis into 1,3-propanediol is reviewed. Unmodified conventional catalysts produces 1,2-propanediol as main product instead of 1,3-propanediol. Most effective catalysts use noble metal as a center for hydrogen activation and tungsten or rhenium as an additive. Pt-WO_3 catalysts on Al-based supports and Ir-ReO_x/SiO_2 catalysts are especially effective in 1,3-propanediol production among the reported materials. Characterization results and proposed reaction mechanisms are also summarized.

Keywords

Heterogeneous catalysis, Hydrogenolysis, Biorefinery, Reducible metal oxide

1. Introduction

Hydrogenolysis reaction is one type of reduction reactions and is composed of dissociation of chemical bonds such as C-C and C-O and hydrogen addition (eqns (1) and (2)).

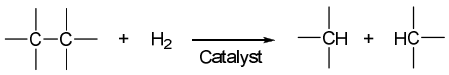

(1)

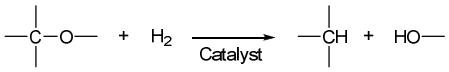

(2)

C-C hydrogenolysis (hydrocracking) decreases the length of the carbon chain and has been widely used in petroleum chemistry.[1] On the other hand, the importance of C-O hydrogenolysis, especially of C-OH bond, is rapidly growing as one method to decrease the oxygen content in the substrate, especially in the area of biomass conversion to fuel or chemicals.[2] This is because shortage of fossil fuels and global warming issues encourage the use of biomass which has generally much higher oxygen content than fossil resources.[3-8]

Glycerol (1,2,3-propanetriol) is manufactured from vegetable oil (triglyceride) as a by-product of soap (eqn 3) and biodiesel fuel (eqn 4).[9]

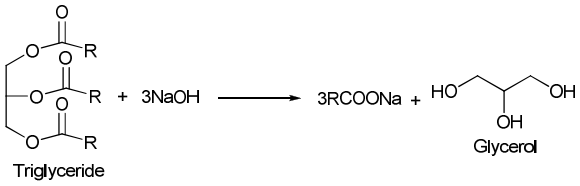

(3)

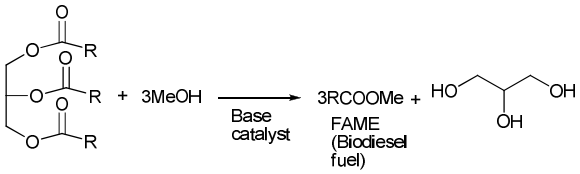

(4)

The amount of glycerol production (> 1 million tons per year) is now much larger than the demand.[9] In the biodiesel production, the disposal of excess glycerol is a problem which

limits the spread of the use of biodiesel. Therefore, conversion of glycerol to useful chemicals has become very important.[10-14] Among various conversion processes of glycerol such as hydrogenolysis, dehydration, oxidation and carboxylation, C-O hydrogenolysis is one of the most promising ones since glycerol has very high oxygen content (O/C=1). Glycerol hydrogenolysis is also important as a model reaction of the reduction of more complicated biomass-related molecules such as sugars.[2,15]

The pathways and products of glycerol hydrogenolysis are summarized in Scheme 1. C-O hydrogenolysis of glycerol first produces 1,2-propanediol (1,2-PrD) and 1,3-propanediol (1,3-PrD). Further C-O hydrogenolysis produces 1-propanol (1-PrOH), 2-propanol (2-PrOH) and finally propane. C-C hydrogenolysis of glycerol or the C-O hydrogenolysis products can give ethylene glycol, ethanol, methanol, ethane and methane. Possible side-reactions include etherification and the reactions with solvents. Among the products, 1,3-PrD is most valuable and is used as a monomer of polypropylene terephthalate (PPT) resin (also named as polytrimethylene terephthalate (PTT)).[13,16] Current 1,3-PrD production methods are fermentation of glucose, hydroformylation of ethylene oxide followed by hydrogenation, and hydration of acrolein followed by hydrogenation. The latter two petroleum-based methods have a problem in selectivity. The global production of 1,3-PrD was in the order of 10^5 t/year. The choice of 1,3-PrD as the target compound is also desirable in view of hydrogen consumption, i.e. glycerol hydrogenolysis to 1,3-PrD consumes only 1 equiv. of hydrogen. However, selective production of 1,3-PrD is very difficult, and most catalytic systems give 1,2-PrD as the main product. Although 1,2-PrD is used as a monomer for polyester resin, an antifreeze agent, a component of paints, and so on, the difference of market price between glycerol and 1,2-PrD is small.[16] Extensive studies have been carried out to develop effective

catalysts for 1,3-PrD productions in these few years. In this paper, we summarize the recent progress on the development of the catalysts and discuss the structural aspects.

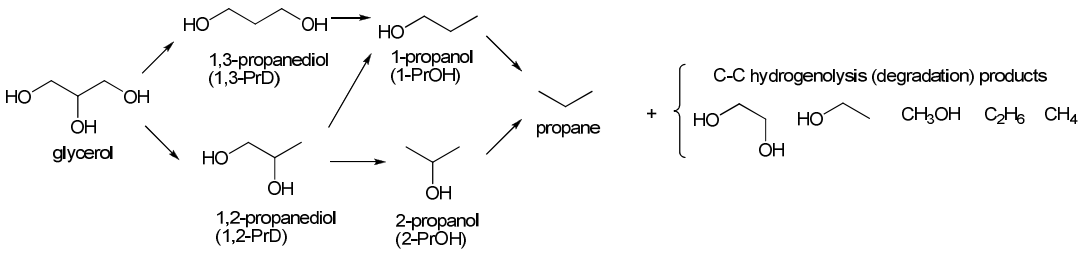

Scheme 1. Pathways and products of glycerol hydrogenolysis

2. Performance of conventional catalytic materials: Mechanism of 1,2-PrD formation

Before introducing the newly developed catalysts for glycerol hydrogenolysis into 1,3-PrD, we discuss the performance of conventional hydrogenation catalysts. Since hydrogenolysis uses hydrogen as one of reactants, catalysts for hydrogenolysis must have an ability to activate hydrogen, similarly to hydrogenation catalysts. Hydrogen is known to be activated over metal surface, and typical metals used are nickel, copper and noble metals.[17,18] As a consequence, various metal catalysts including commercial ones have been tested for glycerol hydrogenolysis. Both batch and flow reactors have been used. The solvent is usually water when batch reactor is used. Examples of results using commercial catalysts are shown in Table 1.[19-22] Several MPa hydrogen pressure and around 473 K reaction temperature are typically applied. Most catalysts give 1,2-PrD as the main product, and very high 1,2-PrD yield can be obtained over Cu catalysts.[19] Formation of C2 compounds is evident over some catalysts, especially over Ru and Ni.[20,21]

--- Insert Table 1 ---

Two types of mechanisms have been proposed by many researchers for glycerol hydrogenolysis into 1,2-PrD (Scheme 2).[16] One is the two-step mechanism composed of dehydration and hydrogenation. The dehydration of glycerol produces acetol (hydroxyacetone), and hydrogenation of acetol gives 1,2-PrD. 1,3-PrD can be produced if the dehydration step produces 3-hydroxypropanal; however, acetol is thermodynamically more stable than 3-hydroxypropanal, leading acetol to the main product in this step. Propanols are by-products of this mechanism. Overreaction of 1,2-PrD produces both propanols, and that of 1,3-PrD produces 1-PrOH. 1-PrOH can be also produced by double-dehydration of glycerol to acrolein and subsequent hydrogenation (eqn 5).

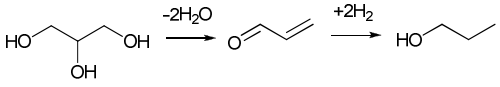

(5)

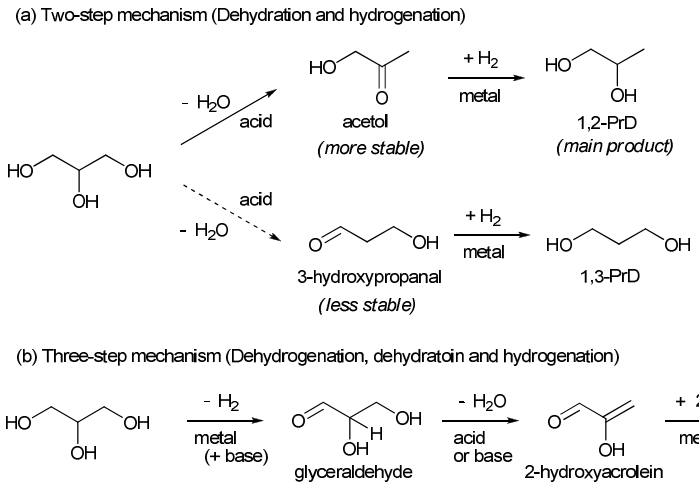

Scheme 2. Mechanisms for 1,2-PrD from glycerol.

Dehydration of glycerol to acrolein has been intensively investigated using strong acid catalysts such as acid-type polyoxometalates, zeolites and mixed metal oxides.[23] Some of these acidic materials have been also used as a component of catalysts for glycerol hydrogenolysis to 1,3-PrOH, as discussed in the next section.

The other mechanism is the three-step one composed of dehydrogenation, dehydration and hydrogenation. Glyceraldehyde, which is formed by dehydrogenation of glycerol, is dehydrated into 2-hydroxyacrolein. Hydrogenation of 2-hydroxyacrolein produces 1,2-PrD. Reactivity of alpha-hydrogen of carbonyl group may be the key: hydrogen and hydroxyl group at alpha and beta-positions, respectively, of carbonyl group are removed during the dehydration step. The formation of ethylene glycol can be explained by the presence retro-aldol reaction of glyceraldehyde (eqn 6).

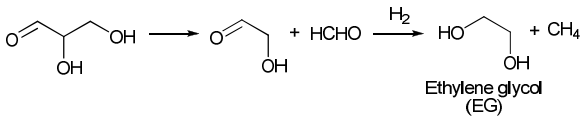

(6)

Addition of acid or base may promote these reaction pathways. Acid catalyzes dehydration reaction, and the two-step mechanism can be promoted. In fact, mixing acidic ion-exchange resin with Ru/C catalyst much increases the activity and 1,2-PrD selectivity.[24-27] The addition of base can promote the dehydrogenation reaction over metal catalysts and can increase the reaction rate via the three-step mechanism. Feng et al. reported that the activity and 1,2-PrD selectivity of Ru/TiO_2 was improved by addition of alkali hydroxide.[28]

There may be other mechanisms for C-O hydrogenolysis than the two-step mechanism or the three-step mechanism. The overall picture of C-O hydrogenolysis mechanism has not been revealed. Nevertheless, it is evident that the reaction route that leads 1,2-PrD, propanols and ethylene glycol such as these two mechanisms should be suppressed in order to obtain high

1,3-PrD yield.

3. Tungsten-added catalysts

The reactants of our reaction are hydrogen and glycerol. While activation of hydrogen can be accomplished by the use of metal catalysts, glycerol is not well activated by metal catalysts. Activation of glycerol by simple acids or bases leads formation of 1,2-PrD, as shown in the previous section. In order to obtain 1,3-PrD selectively, addition of appropriate co-catalyst is necessary. Since the functional group in glycerol is hydroxyl group, potential co-catalyst includes metal oxide that can be strongly interacted with hydroxyl group. Tungsten-based material is one of the most effective co-catalysts for glycerol hydrogenolysis into 1,3-PrD and has been extensively investigated for long time.

3.1. External addition of tungsten species as co-catalyst

Pioneering work of the use of tungsten in glycerol hydrogenolysis was conducted by T. M. Che at Celanese Corporation in 1980s.[29] According to his patent, 1,3-PrD, 1,2-PrD and 1-PrOH can be obtained in 21, 23 and 4% yield, respectively, with $Rh(CO)_2(acac)$ catalyst and H_2WO_4 co-catalyst in 1-methyl-2-pyrrolidinone solvent under synthesis gas (CO/H_2=1/2) at 473 K. When using H_2 alone instead of synthesis gas, slightly lower yield of 1,3-PrD was obtained (yield of 1,3-PrD, 1,2-PrD and 1-PrOH is 13, 20 and 21%, respectively). When sulfuric acid was used instead of H_2WO_4, propanediols and propanols were not formed, indicating that H_2WO_4 plays more role than a simple protic acid. The catalytic performance is sensitive to the amount of H_2WO_4: using twice amount of H_2WO_4 much reduced catalytic activity and the product yields became lower than 1/3.

In 2004, Chaminand et al. used the combination of H_2WO_4 and heterogeneous Rh/C for glycerol hydrogenolysis.[30] High 1,3-PrD/1,2-PrD selectivity ratio (~2) was obtained in sulfolane solvent at 453 K; however, 1,3-PrD selectivity value itself was not high (12%). Water solvent is more favorable than polar organic solvents in view of green chemistry. In water the selectivity to 1,3-PrD became lower (6%) and that to 1,2-PrD was much higher. They also commented that $Rh(CO)_2(acac)$ catalyst with H_2WO_4 co-catalyst was inactive in their conditions with water solvent.

Dam et al. tested the effect of various tungsten-based additives in glycerol hydrogenolysis over commercial catalysts (Pd/SiO_2, Pd/Al_2O_3, Pt/SiO_2 and Pt/Al_2O_3) in water at 473 K.[31] The tested additives were H_2WO_4 and acid-type polyoxometalates, namely phosphotungstic acid ($H_3PW_{12}O_{40}$) and silicotungstic acid ($H_4SiW_{12}O_{40}$). Hydrochloric acid was also tested for comparison. Polyoxometalates are attractive compounds in catalysis, because their chemical properties such as redox potentials, acidities, and solubilities can be tuned by choosing the element compositions and counter cations.[32,33] Acid-type polyoxometalates are soluble in water or other polar solvents and can be used as homogeneous catalysts, while only small amount of H_2WO_4 can be dissolved in water. $H_3PW_{12}O_{40}$ and $H_4SiW_{12}O_{40}$ with Keggin structure are the most typical polyoxotungstates, and the latter is known to be very stable in acidic solution. The results (Fig. 1) showed that considerable amount of 1,3-PrD (20 to 40% selectivity) was formed when tungsten-containing acidic additive and Pt-based catalyst were used. When Pd was used as active metal, the main products were 1,2-PrD and/or 1-PrOH. The types of support and tungsten source have limited influence on the selectivity pattern.

These data show that the combination of noble metal and tungsten is effective in 1,3-PrD formation from glycerol. Based on the electrostatic potential, some tungsten species may well

be reduced in the reaction conditions: $2WO_3 + 2H^+ + 2e^- = W_2O_5 + H_2O$, -0.029 V;[34] $PW_{12}O_{40}^{3-} + e^- = PW_{12}O_{40}^{4-}$, +0.15 V;[35] $SiW_{12}O_{40}^{4-} + e^- = SiW_{12}O_{40}^{5-}$, -0.05 V.[35] Reversible reduction of Pt-supporting $H_4SiW_{12}O_{40}$ with gas-phase H_2 was also reported.[36] It is not known whether or not direct interaction between noble metal and tungsten exists in these systems.

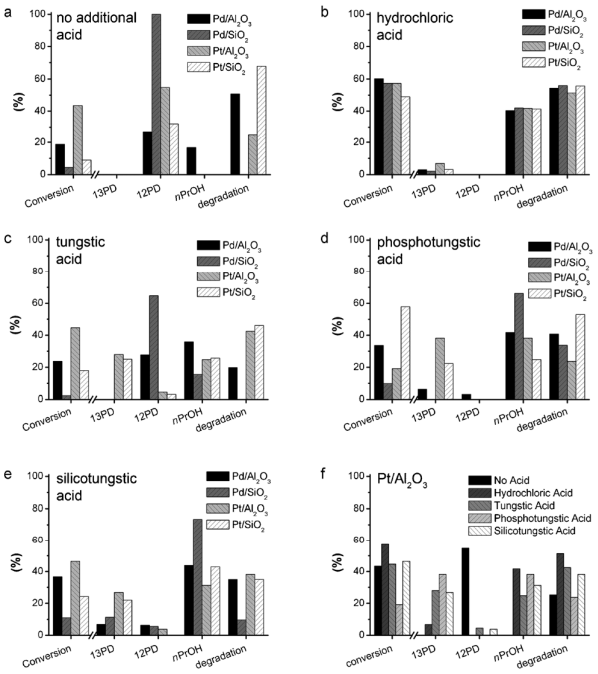

Figure 1. Addition effects of tungsten compounds in Pd- and Pt-based catalysts. PD = propanediol. Conditions: active metal (5 μmol), 100 mM aqueous glycerol (5 mL), additive (HCl, pH 1.5; H_2WO_4, 40 mM; polyacid: 3.5 mM), H_2 (4 MPa), 473 K, 18 h. Reprinted with permission from ref. 31, Copyright (2013) Wiley-VCH.

3.2. Heterogeneous catalysts containing both active metal and polyoxometalate

Heterogeneous catalysts supporting both active metal and polyoxometalate have been investigated by several researchers, since replacement of homogeneous catalysts with

heterogeneous ones can simplify the separation step of catalysts from reaction mixture. In addition, direct interaction between active metal and polyoxometalate is more easily realized in heterogeneous catalysts.

Zhu et al. prepared Cu-$H_4SiW_{12}O_{40}/SiO_2$ catalyst via incipient wetness impregnation method.[37] After calcination at 623 K and reduction at 573 K, the catalyst was applied to vapor-phase hydrogenolysis of glycerol. Conversion and selectivities much depended on the reaction temperature, space velocity, H_2 pressure and initial water content. At the optimum conditions (483 K, 0.54 MPa H_2, without water), conversion and 1,3-PrD selectivity reached 83.4% and 32.1%, respectively. The presence of water decreased both activity and 1,3-PrD selectivity of Cu-$H_4SiW_{12}O_{40}/SiO_2$ catalyst. Later the same group reported aqueous phase glycerol hydrogenolysis over Pt-$H_4SiW_{12}O_{40}/SiO_2$ catalyst with flow reactor.[38] The Pt-$H_4SiW_{12}O_{40}/SiO_2$ catalyst was also prepared via incipient wetness impregnation method and calcined at 623 K. The presence of Keggin structure in the prepared catalyst was verified by Raman spectroscopy. The XRD patterns of reduced catalysts showed that the dispersion of Pt metal was increased with increasing amount of $H_4SiW_{12}O_{40}$. However, the Pt dispersion determined by CO adsorption was first increased and then decreased, probably because of partial covering of the surface Pt metal with polyoxometalate. The XRD patterns showed no peaks for $H_4SiW_{12}O_{40}$, implying the fine dispersion. IR spectra of adsorbed pyridine showed that supporting $H_4SiW_{12}O_{40}$ much increased acid sites, especially Brønsted acid sites. With optimized catalyst and conditions, glycerol conversion and 1,3-PrD selsectivity reached 81.2% and 38.7%, respectively. In the same conditions, Cu-$H_4SiW_{12}O_{40}/SiO_2$ catalyst showed only 9.1% conversion and 8.9% 1,3-PrD selectivity. The same group also reported the catalysis of Pt-$H_4SiW_{12}O_{40}/ZrO_2$ in glycerol hydrogenolysis.[39] Although this study focused on

the production of propanols, good 1,3-PrD selectivity was obtained at lower reaction temperature (~40% selectivity at ~60% conversion and 433 K). Both fresh and spent catalysts showed similar Raman spectra with characteristic bands of $SiW_{12}O_{40}^{4-}$ (950-1020 cm^{-1}), suggesting that the Keggin structure remained intact during the catalysis (Fig. 2). XRD and CO adsorption measurements of fresh and spent catalysts confirmed that the Pt particles on ZrO_2 support had no remarkable agglomeration during the catalysis. The good stability of Pt-$H_4SiW_{12}O_{40}/ZrO_2$ may be due to the strong interaction between acidic $H_4SiW_{12}O_{40}$ and weakly basic sites of ZrO_2 support. Pt-$H_4SiW_{12}O_{40}/ZrO_2$ was further improved by modification with alkali metal.[40] Alkali metals (Li, K, Rb and Cs) were doped into Pt-$H_4SiW_{12}O_{40}/ZrO_2$ by an ion-exchange method using alkali nitrate. The ratio of alkali metal to polyoxometalate was set to 2. Among them, Pt-$Li_2H_2SiW_{12}O_{40}/ZrO_2$ showed higher activity and 1,3-PrD selectivity than unmodified catalyst, attaining 43.5% conversion and 53.6% 1,3-PrD selectivity at 453 K (Scheme 3). The authors pointed out that the modification effect with Li includes adjustment of the acidity and improvement of the tolerance to water solvent.

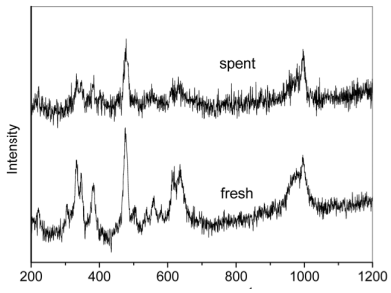

Figure 2. Raman spectra of fresh and spent Pt-$H_4SiW_{12}O_{40}/ZrO_2$ catalysts. Reprinted from ref. 39.

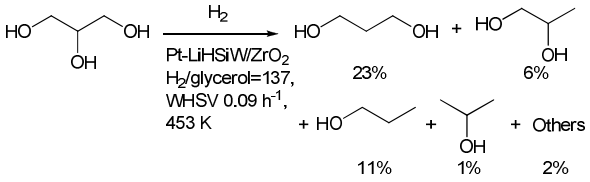

Scheme 3

The use of acid salt of polyoxometalate as a support has been also tested. Kozhevnikov et al. reported glycerol hydrogenolysis over Ru and Rh catalyst supported on $Cs_{2.5}H_{0.5}PW_{12}O_{40}$ [41] which is well known as a water-insoluble strong Brønsted acid with large surface area (~100 m^2 g^{-1}) and good thermal stability (≥773 K).[33,42] The catalysts were prepared by impregnating $Cs_{2.5}H_{0.5}PW_{12}O_{40}$ with metal chloride solution and subsequent reduction with H_2 at 523 K. The catalysts gave high selectivity to 1,2-PrD, while 1,3-PrD was observed only over $Rh/Cs_{2.5}H_{0.5}PW_{12}O_{40}$ (7.1% selectivity). Rapid catalyst deactivation was observed, which was explained by the loss of acidity by reduction of tungsten(VI) in the polyoxometalate. The authors mentioned the possibility that the deactivation will be overcome by using more stable polyoxometalate such as $SiW_{12}O_{40}^{4-}$.

As stated above, the use of polyoxometalate as a component of heterogeneous catalyst can give better 1,3-PrD yield than that of soluble tungsten compound. The advantages of polyoxometalate as catalyst, the ability to tune the properties by changing the constituent elements and counter cations, have been well exploited to develop new catalysts. However, there are too little information about the true active center and reaction mechanism; even it is not known whether the Keggin structure is more effective in glycerol conversion or 1,3-PrD formation than other tungsten structure or not.

3.3. Heterogeneous catalysts with co-supported active metal and tungsten oxide

Supporting active metal on tungsten oxide species is a simple and direct approach to draw out the synergy between active metal catalyst and tungsten co-catalyst. Tungsten oxide is usually first supported on another metal oxide by impregnation and then the precursor of active metal (typically Pt) is impregnated. Supports with large surface area, good stability, and appropriate acid/base property are necessary to obtain good performance.

Kurosaka et al. investigated various noble metal/tungsten/metal oxide support catalysts for glycerol hydrogenolysis in 1,3-dimethyl-2-imidazolidinone (DMI) solvent (Table 2).[43] The catalysts were prepared by sequential impregnation using ammonium metatungstate ($(NH_4)_6H_2W_{12}O_{40}$) and H_2PtCl_6 or metal chloride as precursors. The catalysts were calcined at 773 K after each impregnation. Among the Pt-W catalysts on tested supports (Al-MCM-41, SiO_2-Al_2O_3, Al_2O_3, anatase TiO_2, H-Y zeolite and ZrO_2), Pt/WO_3/ZrO_2 showed the highest activity, 1,3-PrD/1,2-PrD ratio and 1,3-PrD yield (24.2%). Al_2O_3 and SiO_2-Al_2O_3 supports showed relatively good results. The type of noble metal also greatly affects the performance, and Pt showed by far the highest activity and 1,3-PrD/1,2-PrD ratio. The XRD patterns of Pt/WO_3/ZrO_2, Pt/WO_3/Al_2O_3 and Pt/WO_3/SiO_2-Al_2O_3 showed no peaks for Pt or WO_3, while the other Pt/W catalysts with lower performance showed small XRD peaks of Pt and WO_3. These results indicate that the supports should have the ability to keep loaded Pt and WO_3 highly dispersed. On the other hand, all noble metal/WO_3/ZrO_2 catalysts showed no peaks of the noble metal or WO_3, indicating that the catalytic performance was largely affected by the type of noble metal itself.

--- Insert Table 2 ---

Qin et al. applied $Pt/WO_3/ZrO_2$ catalysts for hydrogenolysis of aqueous glycerol.[44] The catalysts were prepared by successive impregnations of $Zr(OH)_4$ with ammonium metatungstate and H_2PtCl_6. The catalysts were calcined at 1023 and 723 K after impregnation with W and Pt, respectively. WO_3/ZrO_2 and $Pt/WO_3/ZrO_2$ prepared by this method are well known solid acids.[45] The presence of WO_3 stabilizes tetragonal ZrO_2 phase, while commercial ZrO_2 has the monoclinic structure. Tungsten is well dispersed onto the ZrO_2 surface as distorted tungsten oxide clusters, except in very high W loadings where bulk WO_3 is formed.[46] Both the amounts of W and Pt much affected the performance (Table 3). The highest activity was obtained when W content was 10 wt%. The authors pointed out that the surface concentration of acid sites on the WO_3/ZrO_2 supports has the maximum when W content was 10 wt%, where the WO_3 loading reached monolayer coverage. The highest 1,3-PrD yield of 32% was obtained using the catalyst with 2 wt% Pt and 10 wt% W. The highest activity of mid-range W loading in WO_3/ZrO_2 catalysts has been also reported for other reactions such as hydrocarbon isomerization.[45]

--- Insert Table 3 ---

Gong et al. prepared a series of $Pt/WO_3/TiO_2/SiO_2$ catalysts with different loadings and applied them to hydrogenolysis of aqueous glycerol.[47] The catalysts were prepared by stepwise impregnation of SiO_2 with tetrabutyl titanate, ammonium metatungstate and H_2PtCl_6. Calcination at 873 K was conducted after each impregnation step. The dependence of catalytic performance on the loading amount of Ti and W showed a volcano-curve (Fig. 3).

The optimal loadings of Ti and W as oxides were 10% and 5%, respectively, and the glycerol conversion and 1,3-PrD selectivity reached 15.3% and 50.5%, respectively. The XRD patterns of $Pt/WO_3/TiO_2/SiO_2$ catalysts showed no peaks of Pt, TiO_2 and WO_3 while those of Pt/SiO_2 and $Pt/WO_3/SiO_2$ showed peaks of Pt. Therefore one role of TiO_2 is to improve the dispersion of Pt. The profiles of temperature-programmed desorption (TPD) of NH_3 and IR spectra of adsorbed pyridine showed that the addition of W enhanced the acidity of catalyst in terms of both acid strength and number of acid site, especially as Brønsted acid sites.

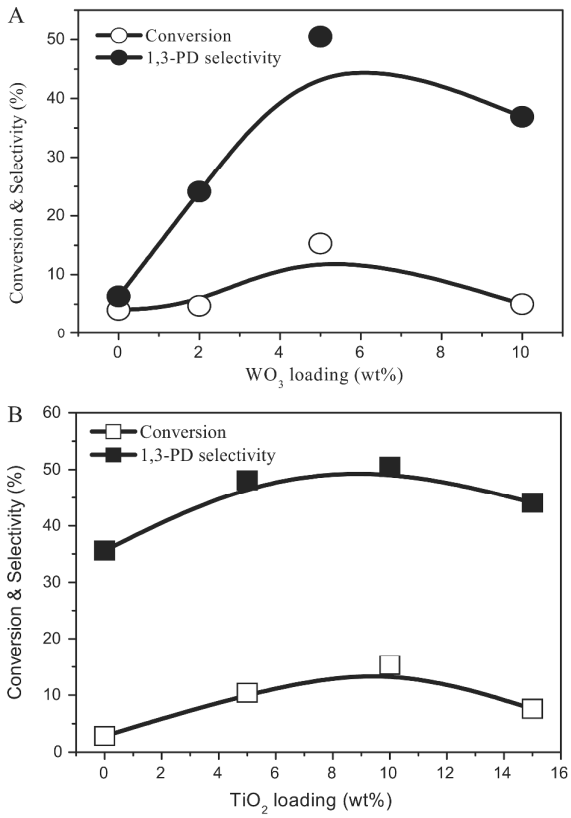

Figure 3. Influence of (A) WO_3 and (B) TiO_2 loadings on $Pt/WO_3/TiO_2/SiO_2$ catalysts for glycerol hydrogenolysis. 1,3-PD = 1,3-propanediol. Reaction conditions: glycerol (4 g), water (36 g), catalyst (2 mL), H_2 (5.5 MPa), 453 K, 12 h. Reprinted with permission from ref. 47,

The combination of Pt, WO_3 and alumina-based supports has been the most successful one for glycerol hydrogenolysis into 1,3-PrD. Suzuki et al. of KAO corporation first invented the combination in 2007.[48] According to their patent, 67% selectivity to 1,3-PrD was obtained at 23% glycerol conversion using Pt(5 wt%)-W(5 wt%)/Al_2O_3 catalyst (Scheme 4). The catalyst was prepared by impregnating commercial Pt/Al_2O_3 with ammonium paratungstate ($(NH_4)_{10}H_2W_{12}O_{42}$) and calcination at 773 K.

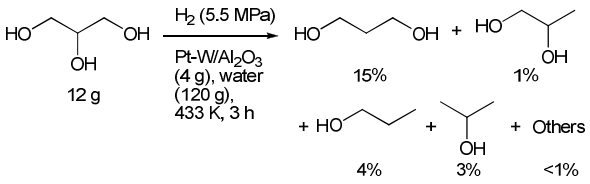

Scheme 4

Very recently, Kaneda et al. has reported a very good result using boehmite (AlOOH) support.[49] The 1,3-PrD yield reached 66-69% from aqueous glycerol (Scheme 5), and these values are the highest in reported ones until now. Tungsten was supported on boehmite by ion-exchange method using aqueous ammonium paratungstate. Almost all tungsten species was attached to the support and the loading amount was set to 8 wt% W. After calcination at 1073 K, the WO_3/"AlOOH" was impregnated with aqueous H_2PtCl_6 by vaporization method to the Pt loading of 1.8 wt%. It should be noted that boehmite was converted into γ-Al_2O_3 phase during the calcination. XRD and W L_3-edge XANES analyses suggested that tungsten (VI) oxide species was highly dispersed on the alumina support. The performance of

Pt/WO_3/"AlOOH" catalyst was compared with that of $Pt/WO_3/Al_2O_3$ which was prepared by the same procedure using γ-Al_2O_3 support with similar surface area to the boehmite. The activity and 1,3-PrD selectivity of $Pt/WO_3/Al_2O_3$ was much lower than that of Pt/WO_3/"AlOOH". The catalysts prepared using boehmite supports with lower surface area (180 → 56 m^2 g^{-1}) showed also lower selectivity to 1,3-PrD (37%). The authors considered that the difference of performance arises from the difference of the number of Al-OH species.

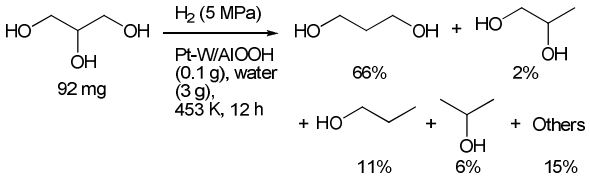

Scheme 5

3.4. Pt catalysts directly supported on tungsten oxides

Tungsten oxides usually have low surface area and are not suitable as supports. However, using tungsten oxide alone as a support certainly leads direct interaction between active metal and tungsten oxide. Tao et al. prepared Pt catalyst supported on mesoporous WO_3 and used it for glycerol hydrogenolysis.[50] The mesoporous WO_3 with surface area of 22 m^2 g^{-1} was prepared by an evaporation-induced self-assembly method using WCl_6 as the precursor and triblock P123 ($EO_{20}PO_{70}EO_{20}$) as the structure-directing agent. The mesoporous structure was confirmed by N_2 adsorption-desorption isotherms and had a pore size distribution centered at 7 nm. Pt was supported on the mesoporous WO_3 calcined at 773 K up to 2 wt% with incipient wetness impregnation method using H_2PtCl_6. After impregnation, the supported Pt catalyst was calcined at 673 K and reduced at 573 K. XRD and TEM analyses showed that Pt metal

was highly dispersed on the mesoporous support, while the catalyst prepared with commercial WO_3 contains larger Pt particles (>10 nm) (Fig. 4). The tungsten oxide phase was partially reduced and formed a "bronze" phase as confirmed by XRD, H_2-TPR (temperature-programmed reduction) and UV-vis spectroscopy. The adsorption band for the "bronze" phase (600-900 nm) was much stronger in Pt/mesoporous WO_3 than in Pt/commercial WO_3. In the glycerol hydrogenolysis, Pt/mesoporous WO_3 catalyst gave 39.3% 1,3-PrD selectivity at 18% conversion. The activity and selectivity were much higher than those of Pt/commercial WO_3 catalyst (29.9% selectivity and 4.5% conversion), and the difference may be related to the high dispersion of Pt and good reducibility of Pt/mesoporous WO_3. Later the same research group reported Pt catalysts supported on mesoporous Ti-W oxides prepared by the similar procedure using $Ti(OBu)_4$ and WCl_6 as precursors.[51] The supports were used after calcination at 773 K, when the Brønsted acid sites were generated. Although the well-ordered honeycomb structure was seriously degraded, the calcined supports still had narrow pore size distributions centered at ~4 nm. The XRD analysis showed that formation of anatase phase proceeded during the calcination. Pt species were highly dispersed when W/Ti molar ratio was below 1. The catalytic activity and 1,3-PrD selectivity of Pt/Ti-W oxide catalysts were similar to those of Pt/mesoporous WO_3.

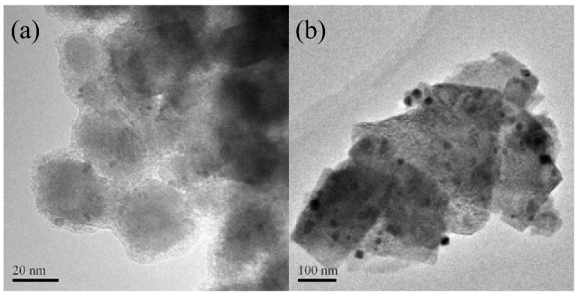

Figure 4. TEM images of Pt/mesoporous WO_3 (a) and Pt/commercial WO_3 (b). Reprinted

with permission from ref. 50 by Editorial Office of Chinese Journal of Catalysis.

Kaneda et al. investigated the addition effect of secondary metal on Pt/WO_3 catalyst.[52] The catalysts were prepared by co-impregnation of commercial WO_3 with mixed solution of H_2PtCl_6 and precursor of additive metal and subsequent calcination at 773 K. The loading amount of Pt and additive was 0.4 and 0.2 wt%, respectively. Among the additive metals tested (Al, V, Cr, Mn, Fe, Zn, Ga, Zr, Mo and Re), Al showed the best effect in the performance in glycerol hydrogenolysis into 1,3-PrD (44% selectivity at 90% conversion). The use of Cr, Mn and Zr resulted in moderate 1,3-PrD yields (25-28% in the same conditions for $Pt\text{-}AlO_x/WO_3$); however, the values were not so different from that obtained over Pt/WO_3 (21%). Addition of V, Fe, Zn, Ga, Mo and Re much decreased the activity. The positive effect of Al may be related to the high performance of Pt-W catalysts on Al-based supports.

3.5. Reaction mechanism over noble metal + tungsten catalysts

The reaction mechanism of 1,3-PrD formation over tungsten-added metal catalysts has not been well understood. Several research groups pointed out the importance of Brønsted acid site in 1,3-PrD formation.[38,41,47,51] The reducibility of tungsten species has been also discussed,[50,51] and the reduction of tungsten with H_2 can produce acidic proton (eqn 7).[45,53]

$$2W^{6+} + H_2 \rightarrow 2W^{5+} + 2H^+ \quad (7)$$

Reaction kinetics, dependence of reactants concentration/partial pressure on the reaction rate, can give important information in determination of reaction mechanism. Large reaction orders (>1) with respect to H_2 pressure were reported for $Pt\text{-}H_4SiW_{12}O_{40}/SiO_2$ and $Pt/WO_3/ZrO_2$ catalysts.[38,44] The kinetics may be related to the formation of 2 equiv. of acidic

proton per one H_2 molecule consumed in the reduction of tungsten. On the other hand, too high H_2 pressure decreased the reaction order for $Pt/WO_3/ZrO_2$,[44] and even volcano-curve dependences on H_2 pressure were reported for $Pt/WO_3/TiO_2/SiO_2$ [47] and $Ru/Cs_{2.5}H_{0.5}PW_{12}O_{40}$ catalysts.[41] Deep reduction of tungsten may lose the catalytic activity. The selectivity to 1,3-PrD was generally gradually increased with increasing H_2 pressure.

One explanation of 1,3-PrD formation is the dehydration-hydrogenation route (Scheme 2(a)). If the dehydration step produces 3-hydroxypropanal instead of acetol, 1,3-PrD should be the main product. It should be noted that the cationic intermediate for 3-hydroxypropanal, secondary carbocation, is more stable than that for acetol, primary carbocation (Scheme 6). Therefore 3-hydroxypropanal formation is kinetically favorable to acetol formation, although thermodynamically unfavorable. Based on this mechanism, the key to high 1,3-PrD is to quickly hydrogenate 3-hydroxypropanal before interconversion between 3-hydroxypropanal and acetol. There is another reason why fast hydrogenation of 3-hydroxypropanal is important: further dehydration of 3-hydroxypropanal produces acrolein, which is a precursor of 1-PrOH. The increase in 1,3-PrD selectivity by increase of H_2 pressure may be due to the increased hydrogenation rate. Stabilizing 3-hydroxypropanal and/or the cationic intermediate can also increase the 1,3-PrD selectivity. In the case of polyoxometalate-based catalysts, the "soft" nature of acidity of polyoxometalate may affect the stability of cationic intermediates. Stabilization of carbocation by slightly reduced WO_x cluster has proposed for $Pt/WO_3/ZrO_2$-catalyzed alkane isomerization.[45] Kaneda et al. proposed the reaction mechanism for Pt-W-Al catalysts (Scheme 7):[52] Glycerol adsorbs on Al-OH site, forming an alkoxide species. Protonation of a secondary hydroxy of the alkoxide and successive dehydration gives a secondary carbocation. The adsorbed carbocation was attacked by

hydride species generated by hydrogen spillover from Pt to WO_3 surface. Hydrolysis of the resultant alkoxide gives 1,3-PrD. In this mechanism, Al-OH site controls the adsorption of glycerol and stabilizes the intermediate. The combination of Pt and WO_3 supplies proton and hydride, and the hydride quickly reduces the intermediate before releasing free 3-hydroxypropanal or acetol. However, there are still undissolved points, such as why Pt and Al work much better than other elements: other noble metal can similarly activate H_2, and many metal cations can form alkoxide structure. Formation of alkoxide on W center in water is also known for some tungsten species with mobile ligands such as aquo, and this property is known to be important in catalytic epoxidation of unsaturated alcohols.[54] Involvement of tungsten alkoxide species in hydrogenolysis cannot be excluded.

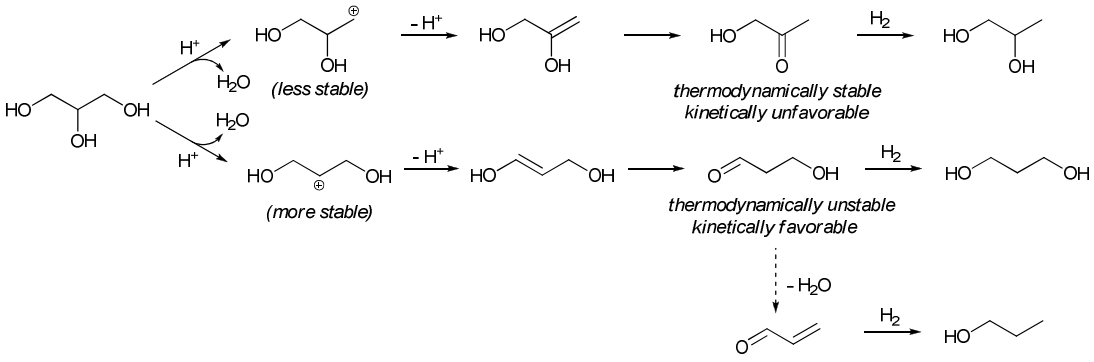

Scheme 6. Elementary reactions in the dehydration of glycerol. Reprinted from ref. 16.

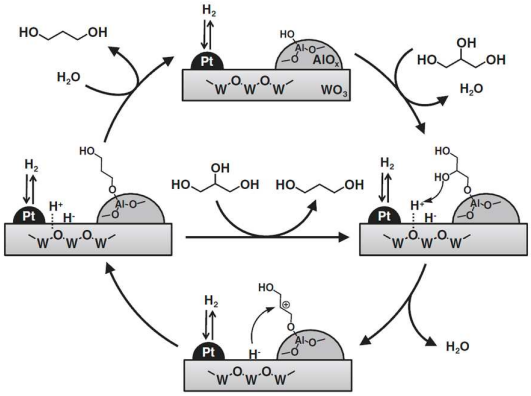

Scheme 7. Mechanism for Pt-Al/WO_3 catalyst proposed by Kaneda et al. Reprinted with permission from ref. 52, Copyright (2012) The Chemical Society of Japan.

4. Rhenium-added catalysts

4.1. Preparation

Rhenium is sometimes an effective additive for noble metal catalysts.[55] Rhenium is located next to tungsten in periodic table, and both elements form metal oxide with d^0 electronic configuration in ambient conditions. The oxides can be reduced to lower valence in reductive conditions. However, the reducibility of tungsten and rhenium is much different: The average valence of W in $W^{VI}O_3$ after reduction is usually larger than +5, and the morphology is not so changed during the reduction at the reaction temperature for glycerol hydrogenolysis (typically ≤473 K). On the other hand, Re^{VII} can be reduced to the average valence of ≤ +4 in the presence of noble metal, and the morphology of rhenium oxide may greatly change during the reduction. It should be also noted that Re_2O_7 is very soluble in water while tungsten oxides or lower valence rhenium oxides are almost insoluble. Therefore, it is difficult to control the structure of rhenium species by changing the preparation methods. The catalysts were usually prepared by impregnation method using aqueous solutions of noble metal

precursor and Re^{VII} precursor such as NH_4ReO_4 and $HReO_4$. The catalysts were calcined and reduced in the reaction conditions or pre-reduced with H_2. Characterization of catalysts should be conducted in the reduced state.

4.2. Ir-ReO_x/SiO_2 catalyst

Ir-ReO_x/SiO_2 catalyst, first reported in 2010,[56] is the most effective one for glycerol hydrogenolysis into 1,3-PrD among Re-added catalysts. Our group compared the catalytic performance of various M^1-ReO_x/SiO_2 (M^1 = Ir, Ru, Rh, Pd and Pt) and Ir-M^2O_x/SiO_2 (M^2 = Re, Cr, Mn, Mo, W and Ag) (Table 4).[57] The precursors used were H_2IrCl_6, H_2PtCl_6, chlorides of the other noble metals, NH_4ReO_4, nitrates of Cr^{III}, Mn^{II}, and Ag^{I}, ammonium heptamolybdate ($(NH_4)_6Mo_7O_{24}$) and ammonium paratungstate. The catalysts were calcined at 773 K after impregnation, and they were reduced in water with 8 MPa H_2 at 473 K just before use. Ir-ReO_x/SiO_2 catalyst was most selective to 1,3-PrD. Rh-ReO_x/SiO_2 showed comparable activity to Ir-ReO_x/SiO_2 based on the number of noble metal, while the 1,3-PrD selectivity was much lower. The other combinations showed lower activity and 1,3-PrD selectivity than Ir-ReO_x/SiO_2. Monometallic Ir/SiO_2 and ReO_x/SiO_2 catalysts were totally inactive.

--- Insert Table 4 ---

The Ir-ReO_x/SiO_2 catalyst showed better performance in the conditions of the Re/Ir molar ratio of 0.25-2, the presence of small amount of acid (such as H_2SO_4 and H-ZSM-5),[56-58] higher glycerol concentration and relatively low temperature (393 K). The H_2 pressure affected the reaction rate, while the effect on the selectivity was very small. Larger Re/Ir ratio

increased the activity, while the selectivity pattern at the same conversion level was almost the same in the Re/Ir range of 0.25-2. The highest 1,3-PrD yield was 38% at 81% conversion (46% selectivity) using the catalyst with 4 wt% Ir and Re/Ir=1 (Scheme 8).[56] The initial selectivity (~70%) was similar to those obtained over optimized Pt-W-Al catalysts; however, the overhydrogenolysis of 1,3-PrD to 1-PrOH lowered the yield over Ir-ReO_x/SiO_2 catalysts. The activity of Ir-ReO_x/SiO_2 was much higher than Pt-W-Al catalysts: Similar rate (~10^1 $mol_{conv\text{-}glycerol}/mol_{Ir\ or\ Pt}$ h^{-1}) was obtained at 393 K and 453 K over Ir-ReO_x/SiO_2 and Pt-W-Al catalyst,[52] respectively.

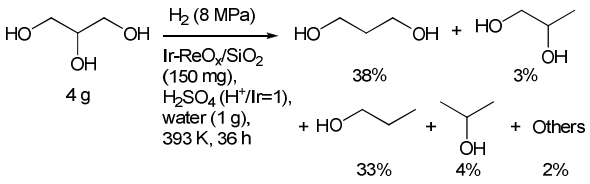

Scheme 8

The Ir-ReO_x/SiO_2 catalyst was characterized with various techniques.[56,57,59] The XRD pattern of unreduced catalyst showed the peaks of IrO_2 as well as SiO_2 support. No peaks of rhenium oxides were observed, suggesting that Re species was highly dispersed. The reduction of Ir-ReO_x/SiO_2 (Re/Ir=1) with H_2 was monitored with H_2-TPR and quick-scanning in situ XAFS. The valence of Re of unreduced catalyst was +7. The reduction of Ir and Re proceeds simultaneously in the range 415-495 K. After the reduction, the average valence of Ir and Re became 0 and +2, respectively, as determined from XANES and EXAFS analysis. The XRD pattern of Ir-ReO_x/SiO_2 after reduction at 495 K had only peaks of Ir metal and SiO_2. The peak of metal (2θ = 40.5°) was not shifted from pure Ir metal, indicating that no

Ir-Re alloy was formed. The average size of Ir metal particles was estimated to be about 2 nm, which was also supported by TEM observation. The curve fitting analysis of Re L_3-edge EXAFS of reduced Ir-ReO_x/SiO_2 showed the presence of both Re-O (0.205 nm) and Re-metal (Ir or Re; 0.273 nm) bonds with coordination number (CN) of 1.6 and 6.5, respectively. The CO adsorption amount on reduced Ir-ReO_x/SiO_2 was significantly smaller than that expected by the Ir metal particle size. It should be noted that CO is adsorbed on Ir metal surface and not on Re oxides. XPS of reduced Ir-ReO_x/SiO_2 showed signal with peaks at 40.7 and 43.3 eV in the Re 4f core level. The peak positions were located between those of Re metal (39.7 and 42.3 eV) and ReO_2 (42.5 and 45.0 eV). Based on these data, we concluded that the surface of Ir metal particles is partially covered with three-dimensional ReO_x clusters. The characterization results of used catalyst were almost identical to those of reduced catalyst in gas phase.

The reduction of Ir/SiO_2 and ReO_x/SiO_2 proceeded in the range 435-555 K and 575-655 K, respectively. The higher reducibility of Ir-ReO_x/SiO_2 than Ir/SiO_2 or ReO_x/SiO_2 suggests the presence of interaction between Ir and Re species even before reduction. The Raman spectrum of unreduced Ir-ReO_x/SiO_2 showed the bands at 1048, 983, 968, 810, 700 and 539 cm^{-1}. The bands at 700 and 539 cm^{-1} were assigned to IrO_2, and those at 810 and 968 cm^{-1} were assigned to ReO_4^- or Re_2O_7. The band at 1048 cm^{-1} was located far from those in reference compounds (NH_4ReO_4, Re_2O_7 and ReO_x/SiO_2; <977 cm^{-1}), and one possible explanation is that the trioxo Re species (-O-Re(=O)$_3$) is formed by the interaction with the IrO_2 surface. The model structures of Ir-ReO_x/SiO_2 in reduced and unreduced states are shown in Fig. 5.

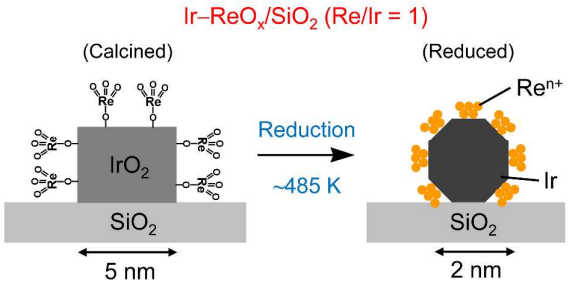

Figure 5. Structural transformation of Ir-ReO_x/SiO_2 during reduction. Reprinted with permission from ref. 59, Copyright (2012) American Chemical Society.

Reaction mechanism of hydrogenolysis over Ir-ReO_x/SiO_2 was investigated with the reactivity trends of related substrates, kinetics and deuterium label study.[56,57,60-63] The C-O bond neighboring terminal OH groups is selectively dissociated: glycerol to 1,3-propanediol,[56-58] erythritol to 1,2,4-butanetriol and 1,4-butanol,[60] 1,2-propanediol to 1-propanol,[56,57] 2-alkoxyethanol to 1:1 mixture of the corresponding alcohol and ethanol,[57] and tetrahydrofurfuryl alcohol to 1,5-pentanediol.[61] Hydrogenolysis of tetrahydrofurfuryl alcohol is especially important, since tetrahydrofurfuryl alcohol can be produced from hemicellulose via furfural as an intermediate.[64-67] Dissociation of C-O bond neighboring secondary OH group is possible with lower reaction rate: 3-hydroxytetrahydrofuran to 1,3-butanediol. The selectivity pattern is different from the order of bond strength: In 2-isopropoxyethanol hydrogenolysis, the $C_{primary}$-O_{ether} bond, which is stronger than the $C_{secondary}$-O_{ether} bond, was selectively dissociated (eqn 8).

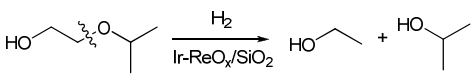

(8)

The reaction order on H_2 pressure was first for these substrates, suggesting that one hydrogen molecule gave one active hydrogen species. The reaction order with respect to

substrate was zero, except substrates with only secondary OH group such as 3-hydroxytetrahydrofuran which gave a positive reaction order.[61-63] The proposed mechanism is shown in Scheme 9. Substrates were adsorbed on Re-OH site with the OH group to form alkoxide species. Hydrogen is activated in the interface between Ir and Re to form hydride species. The C-O bond neighboring the alkoxide group is attacked by the hydride species via S_N2-type reaction. Hydrolysis of produced alkoxide releases the product. The superiority of Ir as an active metal in Re-added catalysts can be related to the nature of active hydrogen species formed on the catalyst. Ir-ReO_x/SiO_2 catalyst is very effective in selective hydrogenation of α,β-unsaturated aldehydes to unsaturated alcohols,[68] where hydride-like reducing agent such as BH_4^- works well. The direct interaction of positively-charged Re with Ir may strengthen the hydride-like nature of hydrogen species formed on Ir. Ir-ReO_x/SiO_2 catalyst is also active in alcohol dehydrogenation such as 1,2-cyclohexanediol to 2-hydroxycyclohexanone, in which reaction heterolytic dissociation of C-H is a key step.[69]

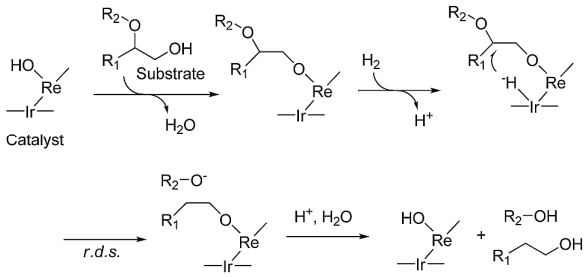

Scheme 9. Proposed mechanism of C-O hydrogenolysis over Ir-ReO_x/SiO_2. Reprinted with permission from ref. 63, Copyright (2013) Elsevier.

Further modification of Ir-ReO_x/SiO_2 can change the catalytic performance. We have tested glycerol hydrogenolysis over Ir-ReO_x/SiO_2 catalyst modified with another metal.[70] Among the

tested elements (B, Na, S, P, Ni, Co, Zn, Cu, Ag, Pd, Pt, Ru and Rh), only Ru and Rh showed a clear positive effect on the catalytic activity. However, the selectivity to 1,3-PrD was slightly decreased. Although the C-O hydrogenolysis activity is decreased, addition of Pd to Ir-ReO_x/SiO_2 enhances the C=C hydrogenation activity and enables one-pot successive conversions of furfural to tetrahydrofurfuryl alcohol (hydrogenation) and tetrahydrofurfuryl alcohol to 1,5-pentanediol (hydrogenolysis).[71] On Ru- or Pd-added Ir-ReO_x/SiO_2 catalysts, EXAFS characterization indicated that both ReO_x-modified Ir particles and ReO_x-modified Ru or Pd particles were separately present.[70,71]

4.3. Rh-ReO_x catalysts

Rh-ReO_x catalysts supported on SiO_2 or carbon are also very active in glycerol hydrogenolysis,[72-74] although less selective to 1,3-PrD than Ir-ReO_x/SiO_2. In contrast to Ir, monometallic Rh catalysts have some activity; however, they are much less active than Rh-ReO_x catalysts (~20 times difference), and 1,3-PrD selectivity is also lower (about half). The dependence of Re amount on the activity of Rh-ReO_x catalysts showed a volcano-curve, and the optimum amount was around Re/Rh=0.5. The Rh-ReO_x catalysts were characterized by XRD, H_2-TPR, CO adsorption, TEM and XAFS.[72,75,76] After reduction at 393 K, Rh and Re in Rh-ReO_x/SiO_2 (Rh 4 wt%, Re/Rh=0.5) was reduced to the metal state and the average valence of around +2, respectively, as determined from H_2-TPR and XANES data. Formation of Rh metal particles was confirmed by XRD and TEM, and the particle size was ~3 nm. CO adsorption amount was smaller than expected for the particle size, similarly to the case of Ir-ReO_x/SiO_2. EXAFS analysis is even more powerful tool than in the case of Ir-ReO_x catalysts because Rh and Re can be clearly distinguished as backscattering atoms. The curve

fitting of Re L_3-edge EXAFS showed the presence of Re-O (CN = 1.4, R = 0.210 nm), Re-Rh (CN = 3.7, R = 0.265 nm) and Re-Re bonds (CN = 2.7; R = 0.272 nm). The Rh-Re bond was also detected by Rh K-edge EXAFS (Rh-Re, CN = 1.8, R=0.265 nm) in addition to Rh-Rh bond (CN=10.1, R=0.267 nm). The characterization data suggest the structure similar to Ir-ReO_x/SiO_2: Rh metal particles with ~3 nm size are covered with low-valent ReO_x clusters (Fig. 6). We obtained similar characterization data for carbon-supported Rh-ReO_x catalysts,[77] while Chia et al. characterized similar Rh-Re/C catalyst with XAFS and proposed the structure with Rh-rich particles with a shell of metallic Re islands.[78] The CO adsorption amount on Rh-ReO_x/SiO_2 was decreased faster with increasing Re amount than on Ir-ReO_x/SiO_2, indicating that Rh surface is more easily covered by ReO_x species. We suppose that ReO_x clusters on Rh metal tend to form monolayer and those on Ir tend to form multilayer structure. The volcano-curve in the activity dependence on Re amount can be explained by the blocking of active Rh sites by excess ReO_x species.

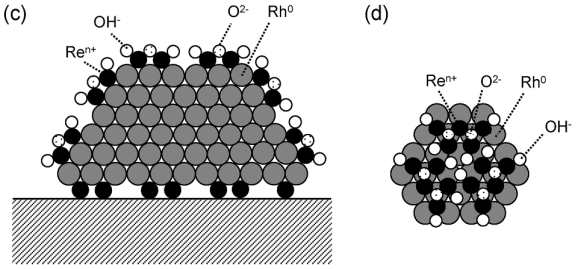

Figure 6. Model structure of Rh-ReO_x/SiO_2 (Re/Rh=0.5) after reduction. (c): Side view, (d): Top view. Reprinted with permission from ref. 76, Copyright (2012) American Chemical Society.

Although not selective in glycerol hydrogenolysis, Rh-ReO_x catalysts are very active and

selective in C-O hydrogenolysis of other substrates: tetrahydrofurfuryl alcohol to 1,5-pentanediol,[71,75,79,80] tetrahydropyran-2-methanol to 1,6-hexanediol,[77-79] 1,2,6-hexanetriol to 1,6-hexanediol,[79,81,82] and 1,2-propanediol to 1-propanol.[74] These reactions are within the type which Ir-ReO_x/SiO_2 catalyst can work for: dissociation of C-O bond neighboring to terminal OH group. Reactions with the mechanism of Ir-ReO_x/SiO_2-catalyzed hydrogenolysis (Scheme 9) can proceed over Rh-ReO_x catalysts; however, other mechanisms that give 1,2-PrD from glycerol also proceed, decreasing 1,3-PrD selectivity of Rh-ReO_x catalysts.

4.4. Other Re-added noble metal catalysts

The addition effect of Re is also evident on Ru catalysts, although the activity and 1,3-PrD selectivity are lower than those of Ir-ReO_x or Rh-ReO_x catalysts. Ma and He conducted detailed investigation on the Ru-Re/SiO_2 catalysts for glycerol hydrogenolysis.[83] The precursors used were $RuCl_3$ and $HReO_4$. The catalysts were calcined at 623 K and reduced in situ in the reaction conditions or with H_2 at 473 K. The H_2-TPR and XRD analyses showed that Re species was mostly in oxidized state after reduction. However, the CO adsorption amount on Ru-Re/SiO_2 was much larger than that on Ru/SiO_2, indicating that covering of Ru with ReO_x species was less severe than in Ir-ReO_x or Rh-ReO_x catalysts. The activity of Ru(3.2 wt%)-Re(3.6 wt%)/SiO_2 catalyst was about three times higher than that of Ru/SiO_2. The difference of selectivity was small between catalysts with and without Re: <10% to 1,3-PrD, ~40% to 1,2-PrD and ~30% to 1-PrOH. The promotion of activity by Re addition can be explained by increased Ru dispersion.

Daniel et al. reported the performance of Pt-Re/C and the detailed characterization using XAFS.[84] The precursors used were H_2PtCl_6 and $HReO_4$, and the loading amount was set to 5

wt% Pt and 4.9 wt% Re. After impregnation, the dried catalysts were reduced with H_2 at 773 K or 973 K. The catalyst reduced at higher temperature was more selective to 1,3-PrD, and 34% selectivity was obtained at 20% conversion and 443 K. The sintering during the reduction at high temperature was not severe: particles with average size of 1.2 and 1.7 nm (TEM analysis) were present on the samples reduced at 773 and 973 K, respectively. The authors commented that the increase in 1,3-PrD selectivity by higher reduction temperature might be resulted from a higher level of Re incorporation into the bimetallic Pt-Re particles. The Re L_3-edge XANES analysis showed that the average Re valence was ~+2 in both catalysts reduced at 773 K or 973 K. The authors proposed the structure where Pt-Re bimetallic particles and oxidized Re species were separately present. Formation of Pt-Re alloy particles has been proposed for Pt-Re/Al_2O_3 catalyst which is well known to be active in naphtha reforming.[55,85] On the other hand, we characterized Pt-ReO_x/SiO_2 catalysts (Pt 2 wt%, Re/Pt=0.2 or 0.5) with H_2-TPR, XAFS and CO adsorption, and we concluded that Pt metal particles were covered with small ReO_x clusters.[86,87]

Pd catalysts are inactive in glycerol hydrogenolysis regardless of whether Re is added or not (Tables 1 and 4). Nevertheless, loading of Pd promotes the reduction of Re species loaded on the same support, similarly to the loading of other noble metals. Pd-ReO_x catalysts show higher activity in reactions catalyzed by reduced Re species such as hydrogenation of carboxylic acid than monometallic Re catalysts.[88]

5. Other catalysts for 1,3-PrD formation from glycerol

There are few reports that present effective catalysts for 1,3-PrD formation from glycerol without use of tungsten or rhenium. Among Ir/SiO_2 catalysts modified with additional metal,

the ones modified with Mo or V showed some activity to 1,3-PrD formation (Table 4); however, the activity and 1,3-PrD selectivity were lower than those of Ir-ReO_x/SiO_2. Rh-MoO_x/SiO_2 catalyst, which is a good catalyst for hydrogenolysis of tetrahydrofurfuryl alcohol to 1,5-pentanediol like Rh-ReO_x/SiO_2,[89,90] showed even lower 1,3-PrD selectivity than Rh/SiO_2.[72] Oh et al. reported very selective 1,3-PrD formation using Pt-sulfated zirconia.[91] Sulfated zirconia is a well-known "super acid". The sulfated zirconia was prepared by sol-gel method using $Zr(OBu)_4$ solution in 1-propanol and aqueous H_2SO_4. After calcination at 898 K, it was impregnated with H_2PtCl_6 and calcined again at 773 K. The loading amount of Pt was 2 wt%. Using this catalyst, impressive 84% 1,3-PrD selectivity was observed at 66.5% glycerol conversion in 1,3-dimethyl-2-imidazolidinone (DMI) solvent (Scheme 10).

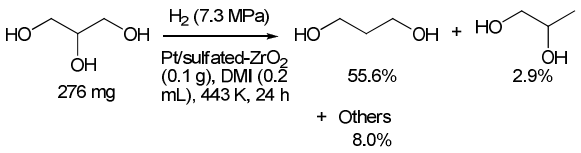

Scheme 10

Interestingly, blank experiment without catalyst in the same conditions also produced significant amount of 1,3-PrD (7.6% yield, 23.7% glycerol conversion). The DMI solvent might play an essential role.

6. Conclusions and outlook

Most effective catalysts for 1,3-PrD production from glycerol contain both noble metal and

tungsten or rhenium. Noble metal is required to activate hydrogen molecule. The role of tungsten or rhenium is not well understood and may be different in different catalysts. The possible roles include: supplying Brønsted acid sites, binding and activating glycerol molecule, working as a carrier of active hydrogen species by partial reduction, and modifying the electronic states of noble metal by direct interaction with noble metal atom. Recent progress in catalyst development enables the production of 1,3-PrD in >50% selectivity. Tungsten-added catalysts can give high 1,3-PrD yield, especially with those containing Pt, W and Al. However, the catalytic performance is very sensitive to the structure and compositions. The activity of Pt-W based catalysts may also need to be improved. Further refinement in preparation methods or compositions may well lead better catalysts. Rhenium-added catalysts are attractive as catalysts with high activity. The best catalyst, namely Ir-ReO_x/SiO_2, shows good 1,3-PrD selectivity at low conversion. However, overhydrogenolysis lowers the 1,3-PrD yield at higher conversion. To develop new catalysts, attention should be paid to the dynamic change in the structure of Re species during the reduction. Because of this point, it is difficult to control the structure except by changing the composition. After all, developing new additional promotors or new methods to control the structure will improve the catalytic performance of both types of catalysts using tungsten or rhenium.

References

[1] J. Weitkamp, *ChemCatChem*, 2012, **4**, 292-306.

[2] A. M. Ruppert, K. Weinberg and R. Palkovits, *Angew. Chem. Int. Ed.*, 2012, **51**, 2564-2601.

[3] A. Corma, S. Iborra and A. Velty, *Chem. Rev.*, 2007, **107**, 2411-2502.

[4] J. J. Bozell and G. R. Petersen, *Green Chem.*, 2010, **12**, 539-554.

[5] A. J. Ragauskas, C. K. Williams, B. H. Davison, G. Britovsek, J. Cairney, C. A. Eckert, W. J. Frederick Jr., J. P. Hallett, D. J. Leak, C. L. Liotta, J. R. Mielenz, R. Murphy, R. Templer and T. Tschaplinski, *Science*, 2006, **311**, 484-489.

[6] J. N. Chheda, G. W. Huber and J. A. Dumesic, *Angew. Chem. Int. Ed.*, 2007, **46**, 7164-7183.

[7] M. Schlaf, *Dalton Trans.*, 2006, 4645-4653.

[8] M. Besson, P. Gallezot and C. Pinel, *Chem. Rev.*, DOI: 10.1021/cr4002269.

[9] C.-H. Zhou, J. N. Beltramini, Y.-X. Fan and G. Q. Lu, *Chem. Soc. Rev.*, 2008, **37**, 527-549.

[10] M. Pagliaro, R. Ciriminna, H. Kimura, M. Rossi and C. D. Pina, *Angew. Chem. Int. Ed.*, 2007, **46**, 4434-4440.

[11] G. P. da Silva, M. Mack and J. Contiero, *Biotechnol. Adv.*, 2009, **27**, 30-39.

[12] D. T. Johnson and K. A. Taconi, *Environ. Prog.*, 2007, **26**, 338-348.

[13] A. Behr, J. Eilting, K. Irawadi, J. Leschinski and F. Lindner, *Green Chem.*, 2008, **10**, 13-30.

[14] C. H. Zhou, H. Zhao, D. S. Tong, L. M. Wu and W. H. Yu, *Catal. Rev. Sci. Eng.*, 2013, **55**, 369-453.

[15] J. W. Medlin, *ACS Catal.*, 2011, **1**, 1284-1297.

[16] Y. Nakagawa and K. Tomishige, *Catal. Sci. Technol.*, 2011, **1**, 179-190.

[17] V. Ponec, *Appl. Catal. A*, 1997, **149**, 27-48.

[18] P. Mäki-Arvela, J. Hájek, T. Salmi and D. Y. Murzin, *Appl. Catal. A*, 2005, **292**, 1-49.

[19] M. A. Dasari, P.-P. Kiatsimkul, W. R. Sutterlin and G. J. Suppes, *Appl. Catal. A*, 2005, **281**, 225-231.

[20] S. R. Schmidt, S. K. Tanielyan, N. Marin, G. Alvez and R. L. Augustine, *Top. Catal.*, 2010, **53**, 1214-1216.

[21] A. Perosa and P. Tundo, *Ind. Eng. Chem. Res.*, 2005, **44**, 8535-8537.

[22] I. Furikado, T. Miyazawa, S. Koso, A. Shimao, K. Kunimori and K. Tomishige, *Green Chem.*, 2007, **9**, 582-588.

[23] B. Katryniok, S. Paul, V. Bellière-Baca, P. Ray and F. Dumeignil, *Green Chem.*, 2010, **12**, 2079-2098.

[24] Y. Kusunoki, T. Miyazawa, K. Kunimori and K. Tomishige, *Catal. Commun.*, 2005, **6**, 645-649.

[25] T. Miyazawa, Y. Kusunoki, K. Kunimori and K. Tomishige, *J. Catal.*, 2006, **240**, 213-221.

[26] T. Miyazawa, S. Koso, K. Kunimori and K. Tomishige, *Appl. Catal. A*, 2007, **318**, 244-251.

[27] T. Miyazawa, S. Koso, K. Kunimori and K. Tomishige, *Appl. Catal. A*, 2007, **329**, 30-35.

[28] J. Feng, J. Wang, Y. Zhou, H. Fu, H. Chen and X. Li, *Chem. Lett.*, 2007, **36**, 1274-1275.

[29] T. M. Che, *US Pat.* US 4642394 to Celanese Corp., 1987.

[30] J. Chaminand, L. Djakovitch, P. Gallezot, P. Marion, C. Pinel and C. Rosier, *Green Chem.*, 2004, **6**, 359-361.

[31] J. ten Dam, K. Djanashvili, F. Kapteijn and U. Hanefeld, *ChemCatChem*, 2013, **5**, 497-505.

[32] C. L. Hill, *Chem. Rev.*, 1998, **98**, 1-390.

[33] T. Okuhara, N. Mizuno and M. Misono, *Adv. Catal.*, 1996, **41**, 113-252.

[34] *CRC Handbook of Chemistry and Physics on DVD*, ed. W. M. Haynes, CRC Press,

Version 2012, 2012.

[35] I. V. Kozhevnikov and K. I. Matveev, *Appl. Catal.*, 1983, **5**, 135-150.

[36] S. Itagaki, K. Yamaguchi and N. Mizuno, *Chem. Mater.*, 2011, **23**, 4102-4104.

[37] L. Huang, Y. Zhu, H. Zheng, G. Ding and Y. Li, *Catal. Lett.*, 2009, **131**, 312-320.

[38] S. Zhu, Y. Zhu, S. Hao, L. Chen, B. Zhang and Y. Li, *Catal. Lett.*, 2012, **142**, 267-274.

[39] S. Zhu, Y. Zhu, S. Hao, H. Zheng, T. Mo and Y. Li, *Green Chem.*, 2012, **14**, 2607-2616.

[40] S. Zhu, X. Gao, Y. Zhu, Y. Zhu, X. Xiang, C. Hu and Y. Li, *Appl. Catal. B*, 2013, **140-141**, 60-67.

[41] A. Alhanash, E. F. Kozhevnikova and I. V. Kozhevnikov, *Catal. Lett.*, 2008, **120**, 307-311.

[42] T. Nakato, M. Kimura, S.-I. Nakata and T. Okuhara, *Langmuir*, 1998, **14**, 319-325.

[43] T. Kurosaka, H. Maruyama, I. Naribayashi and Y. Sasaki, *Catal. Commun.*, 2008, **9**, 1360-1363.

[44] L.-Z. Qin, M.-J. Song and C.-L. Chen, *Green Chem.*, 2010, **12**, 1466-1472.

[45] D. G. Barton, S. K. Soled, G. D. Meitzner, G. A. Fuentes and E. Iglesia, *J. Catal.*, 1999, **181**, 57-72.

[46] E. I. Ross-Medgaarden, W. V. Knowles, T. Kim, M. S. Wong, W. Zhou, C. J. Kiely and I. E. Wachs, *J. Catal.*, 2008, **256**, 108-125.

[47] L. Gong, Y. Lu, Y. Ding, R. Lin, J. Li, W. Dong, T. Wang and W. Chen, *Appl. Catal. A*, 2010, **390**, 119-126.

[48] N. Suzuki, Y. Yoshikawa, M. Takahashi and M. Tamura, *World Pat.* WO 2007129560 to KAO Corporation, 2007.

[49] R. Arundhathi, T. Mizugaki, T. Mitsudome, K. Jitsukawa and K. Kaneda, *ChemSusChem*,

2013, **6**, 1345-1347.

[50] L. Liu, Y. Zhang, A. Wang and T. Zhang, *Chin. J. Catal.*, 2012, **33**, 1257-1261.

[51] Y. Zhang, X.-C. Zhao, Y. Wang, L. Zhou, J. Zhang, J. Wang, A. Wang and T. Zhang, *J. Mater. Chem. A*, 2013, **1**, 3724-3732.

[52] T. Mizugaki, T. Yamakawa, R. Arundhathi, T. Mitsudome, K. Jitsukawa and K. Kaneda, *Chem. Lett.*, 2012, **41**, 1720-1722.

[53] T. Baba, Y. Hasada, M. Nomura, Y. Ohno and Y. Ono, *J. Mol. Catal. A*, 1996, **114**, 247-255.

[54] K. Kamata, K. Yamaguchi and N. Mizuno, *Chem. Eur. J.*, 2004, **10**, 4728-4734.

[55] J. Xiao and R. J. Puddephatt, *Coord. Chem. Rev.*, 1995, **143**, 457-500.

[56] Y. Nakagawa, Y. Shinmi, S. Koso and K. Tomishige, *J. Catal.*, 2010, **272**, 191-194.

[57] Y. Amada, Y. Shinmi, S. Koso, T. Kubota, Y. Nakagawa and K. Tomishige, *Appl. Catal. B*, 2011, **105**, 117-127.

[58] Y. Nakagawa, X. Ning, Y. Amada and K. Tomishige, *Appl. Catal. A*, 2012, **433-434**, 128-134.

[59] Y. Amada, H. Watanabe, M. Tamura, Y. Nakagawa, K. Okumura and K. Tomishige, *J. Phys. Chem. C*, 2012, **116**, 23503-23514.

[60] Y. Amada, H. Watanabe, Y. Hirai, Y. Kajikawa, Y. Nakagawa and K. Tomishige, *ChemSusChem*, 2012, **5**, 1991-1999.

[61] K. Chen, K. Mori, H. Watanabe, Y. Nakagawa and K. Tomishige, *J. Catal.*, 2012, **294**, 171-183.

[62] K. Chen, M. Tamura, Z. Yuan, Y. Nakagawa and K. Tomishige, *ChemSusChem*, 2013, **6**, 613-621.

[63] Y. Nakagawa, K. Mori, K. Chen, Y. Amada, M. Tamura and K. Tomishige, *Appl. Catal. A*, 2013, **468**, 418-425.

[64] Y. Nakagawa, M. Tamura and K. Tomishige, *ACS Catal.*, 2013, **3**, 2655-2668.

[65] Y. Nakagawa and K. Tomishige, *Catal. Commun.*, 2010, **12**, 154-156.

[66] Y. Nakagawa, H. Nakazawa, H. Watanabe and K. Tomishige, *ChemCatChem*, 2012, **4**, 1791-1797.

[67] Y. Nakagawa and K. Tomishige, *Catal. Today*, 2012, **195**, 136-143.

[68] M. Tamura, K. Tokonami, Y. Nakagawa and K. Tomishige, *Chem. Commun.*, 2013, **49**, 7034-7036.

[69] H. Sato, M. Tamura, Y. Nakagawa and K. Tomishige, *Chem. Lett.*, DOI: 10.1246/cl.130983.

[70] M. Tamura, Y. Amada, S. Liu, Z. Yuan, Y. Nakagawa and K. Tomishige, *J. Mol. Catal. A*, DOI: 10.1016/j.molcata.2013.09.015.

[71] S. Liu, Y. Amada, M. Tamura, Y. Nakagawa and K. Tomishige, *Green Chem.*, DOI: 10.1039/c3gc41335g.

[72] Y. Shinmi, S. Koso, T. Kubota, Y. Nakagawa and K. Tomishige, *Appl. Catal. B*, 2010, **94**, 318-326.

[73] A. Shimao, S. Koso, N. Ueda, Y. Shinmi, I. Furikado and K. Tomishige, *Chem. Lett.*, 2009, **38**, 540-541.

[74] Y. Amada, S. Koso, Y. Nakagawa and K. Tomishige, *ChemSusChem*, 2010, **3**, 728-736.

[75] S. Koso, I. Furikado, A. Shimao, T. Miyazawa, K. Kunimori and K. Tomishige, *Chem. Commun.*, 2009, 2035-2037.

[76] S. Koso, H. Watanabe, K. Okumura, Y. Nakagawa and K. Tomishige, *J. Phys. Chem. C*,

2012, **116**, 3079-3090.

[77] K. Chen, S. Koso, T. Kubota, Y. Nakagawa and K. Tomishige, *ChemCatChem*, 2010, **2**, 547-555.

[78] M. Chia, B. J. O'Neill, R. Alamillo, P. J. Dietrich, F. H. Ribeiro, J. T. Miller and J. A. Dumesic, *J. Catal.*, 2013, **308**, 226-236.

[79] M. Chia, Y. J. Pagán-Torres, D. Hibbitts, Q. Tan, H. N. Pham, A. K. Datye, M. Neurock, R. J. Davis and J. A. Dumesic, *J. Am. Chem. Soc.*, 2011, **133**, 12675-12689.

[80] Y. Nakagawa and K. Tomishige, *Catal. Surv. Asia*, 2011, **15**, 111-116.

[81] T. Buntara, S. Noel, P. H. Phua, I. Melián-Cabrera, J. G. de Vries and H. J. Heeres, *Top. Catal.*, 2012, **55**, 612-619.

[82] T. Buntara, I. Melián-Cabrera, Q. Tan, J. L. G. Fierro, M. Neurock, J. G. de Vries and H. J. Heeres, *Catal. Today*, 2013, **210**, 106-116.

[83] L. Ma and D. He, *Catal. Today*, 2010, **149**, 148-156.

[84] O. M. Daniel, A. DeLaRiva, E. L. Kunkes, A. K. Datye, J. A. Dumesic and R. J. Davis, *ChemCatChem*, 2010, **2**, 1107-1114.

[85] J. Sá, C. Kartusch, M. Makosch, C. Paun, J. A. van Bokhoven, E. Kleymenov, J. Szlachetko, M. Nachtegaal, H. G. Manyar and C. Hardacre, *Chem. Commun.*, 2011, **47**, 6590-6592.

[86] T. Ebashi, Y. Ishida, Y. Nakagawa, S. Ito, T. Kubota and K. Tomishige, *J. Phys. Chem. C*, 2010, **114**, 6518-6526.

[87] Y. Ishida, T. Ebashi, S. Ito, T. Kubota, K. Kunimori and K. Tomishige, *Chem. Commun.*, 2009, 5308-5310.

[88] Y. Takeda, Y. Nakagawa and K. Tomishige, *Catal. Sci. Technol.*, 2012, **2**, 2221-2223.

[89] S. Koso, N. Ueda, Y. Shinmi, K. Okumura, T. Kizuka and K. Tomishige, *J. Catal.*, 2009, **267**, 89-92.

[90] S. Koso, H. Watanabe, K. Okumura, Y. Nakagawa and K. Tomishige, *Appl. Catal. B*, 2012, **111-112**, 27-37.

[91] J. Oh, S. Dash and H. Lee, *Green Chem.*, 2011, **13**, 2004-2007.

Table 1. Selected examples of glycerol hydrogenolysis into 1,2-PrD over commercial catalysts[a]

Catalyst	H_2 [MPa]	Glycerol/water/catalyst [g]	Temp. [K]	Time [h]	Conv. [%]	Products (selectivity [%])	ref.
Copper chromite	2.1	50/10/2.5	473	24	65.3	1,2-PrD (89.6)	19
Pt/C, 5 wt%	1.38	50/10/2.5	473	24	34.6	1,2-PrD (82.7)	19
Pd/C, 5 wt%	1.38	50/10/2.5	473	24	5	1,2-PrD (72.0)	19
Ru/C, 5 wt%	1.38	50/10/2.5	473	24	43.7	1,2-PrD (40.0)	19
Ni/C	1.38	50/10/2.5	473	24	39.8	1,2-PrD (68.6)	19
RANEY® Cu	1.4	H_2/20 wt% glycerol=375/0.05[b]	478	LHSV=0.043 h^{-1}	100	1,2-PrD (94), EG (1.6)	20
RANEY® Ni	1	8/0/2	463	44	97	1,2-PrD (71), ethanol (19), CO_2 (10)	21
Ru/C, 5 wt%	8	4/16/0.15	393	10	3.5	1,2-PrD (26), 1,3-PrD (5), 1-PrOH (27), EG (22), ethanol (6), CH_4 (12)	22
Rh/C, 5 wt%	8	4/16/0.15	393	10	1.9	1,2-PrD (63), 1,3-PrD (7), 1-PrOH (19), 2-PrOH (7), EG (2), ethanol (1), CH_4 (1)	22

[a] PrD = propanediol, EG = ethylene glycol, PrOH = propanol. [b] Ratio by volume.

Table 2. Glycerol hydrogenolysis over supported noble metal-WO_3 catalysts in DMI (ref. 43)[a]

Catalyst	Conv. [%]	Selectivity [%]		
		1,3-PrD	1,2-PrD	1-PrOH
No catalyst	<3	n.d.	n.d.	n.d.
$Pt/WO_3/TiO_2$	19	35	38	27
$Pt/WO_3/HY$	26	28	34	19
$Pt/WO_3/AlMCM\text{-}41$	28	27	25	26
$Pt/WO_3/SiO_2\text{-}Al_2O_3$	42	26	27	23
$Pt/WO_3/Al_2O_3$	44	30	25	26
$Pt/WO_3/ZrO_2$	86	28	15	32
$Pd/WO_3/ZrO_2$	24	20	28	20
$Rh/WO_3/ZrO_2$	86	5	33	16
$Ru/WO_3/ZrO_2$	47	7	19	17
$Ir/WO_3/ZrO_2$	22	14	31	16

[a] DMI = 1,3-dimethyl-2-imidazolidinone, PrD = propanediol, PrOH = propanol, n.d. = not detected. Reaction conditions: glycerol (3 mmol), DMI (0.2 mL), catalyst (100 mg; noble metal 2 wt%, WO_3 19.6%), H_2 (8 MPa), 443 K, 18 h.

Table 3. Glycerol hydrogenolysis over $Pt/WO_3/ZrO_2$ catalysts in water (ref. 44)[a]

Metal loadings [wt%]		Conv.	Selectivity [%]			
Pt	W	[%]	1,3-PrD	1,2-PrD	1-PrOH	2-PrOH
1	10	14.2	36	4.2	50	9.9
2	10	41.6	44	3.6	44	8.2
3	10	70.2	46	2.6	44	7.6
4	10	84.5	26	0.7	67	6.3
2	5	27.0	44	9.3	38	7.8
2	15	29.9	36	6.4	48	9.7

[a] PrD = propanediol, PrOH = propanol. Reaction conditions: glycerol (60 wt% aq., 0.5 mL h^{-1}), catalyst (2 mL; calcination temperature for support: 1073 K), H_2 (4 MPa, 10 mL min^{-1}), 403 K, after 24 h.

Table 4. Glycerol hydrogenolysis over Ir-ReO_x/SiO_2 and the related catalysts (ref. 57)[a]

Catalyst	Conv. [%]	Selectivity [%]				
		1,3-PrD	1,2-PrD	1-PrOH	2-PrOH	Others
Ir-ReO_x/SiO_2	22.6	65	8.2	19	8.0	0.3
Rh-ReO_x/SiO_2	28.9	19	27	36	16	1.9
Ru-ReO_x/SiO_2	26.1	12	52	22	3.7	11
Pt-ReO_x/SiO_2	2.1	40	21	29	9	1
Pd-ReO_x/SiO_2	<0.1	n.d.	n.d.	n.d.	n.d.	n.d.
Ir-MoO_x/SiO_2	4.7	24	55	11	8.6	0.7
Ir-WO_x/SiO_2	2.7	49	19	20	10	1
Ir-VO_x/SiO_2	0.4	39	59	n.d.	n.d.	2
Ir-CrO_x/SiO_2	<0.1	n.d.	n.d.	n.d.	n.d.	n.d.
Ir-MnO_x/SiO_2	<0.1	n.d.	n.d.	n.d.	n.d.	n.d.
Ir-Ag/SiO_2	<0.1	n.d.	n.d.	n.d.	n.d.	n.d.

[a] PrD = propanediol, PrOH = propanol, n.d. = not detected. Reaction conditions: glycerol (4 g), water (2 g), catalyst (150 mg; noble metal 4 wt%, additive/noble metal=0.25; reduced at 473 K), H_2SO_4 (H^+/additive =1), H_2 (8 MPa), 393 K, 12 h.

Table of contents entry

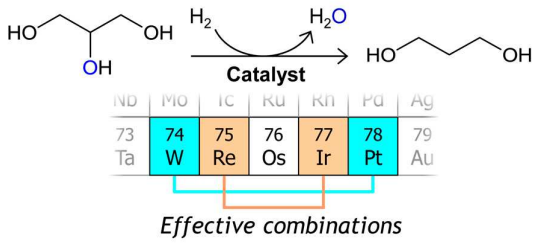

The combinations of Pt-W and Ir-Re can catalyze the hydrogenolysis of glycerol to 1,3-propanediol in high selectivity.